

Self-modulated band gap in boron nitride nanoribbons and hydrogenated sheets

Zhuhua Zhang^{a,b}, Wanlin Guo^a, and Boris I. Yakobson^b

^aState Key Laboratory of Mechanics and Control of Mechanical Structures, Key Laboratory for Intelligent Nano Materials and Devices of Ministry of Education and Institute of Nano Science, Nanjing University of Aeronautics and Astronautics, Nanjing 210016, China.

^bDepartment of Mechanical Engineering and Materials Science, Rice University, Houston, Texas 77005, USA;

Email: zz19@rice.edu

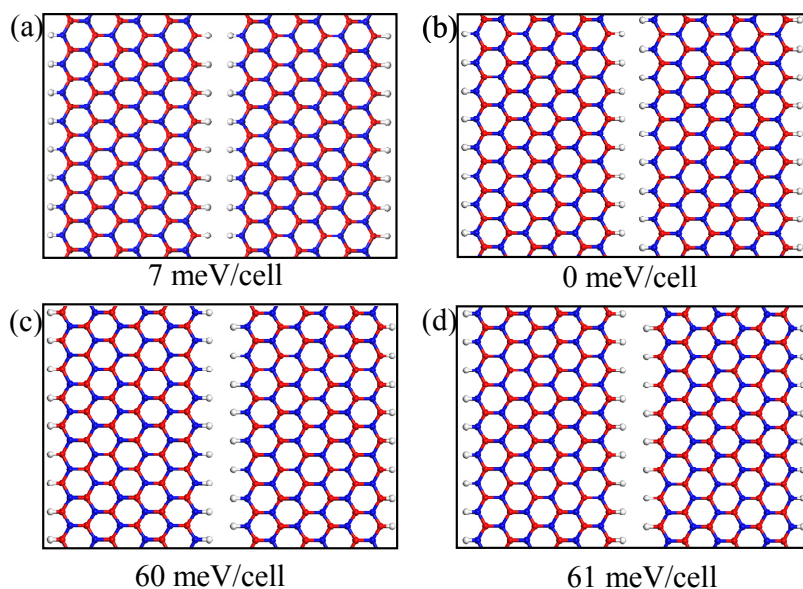


Fig. S1 The 6-ZBNR-2 with different interface structures. (a) B-edge versus N-edge, with well-aligned edge H atoms, (b) B-edge versus N-edge, with misaligned edge H atoms, (c) N-edge versus N-edge and (d) B-edge versus B-edge. The number below each figure is the relative energy with respect to the structure in (b).

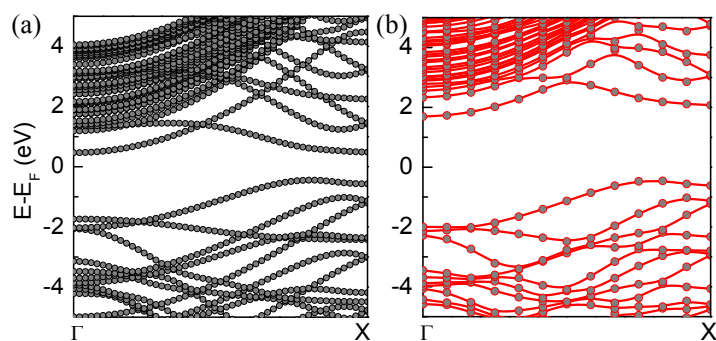


Fig. S2 (a) GGA and (b) HSE06 band structures of the 3-ZBNR-3.

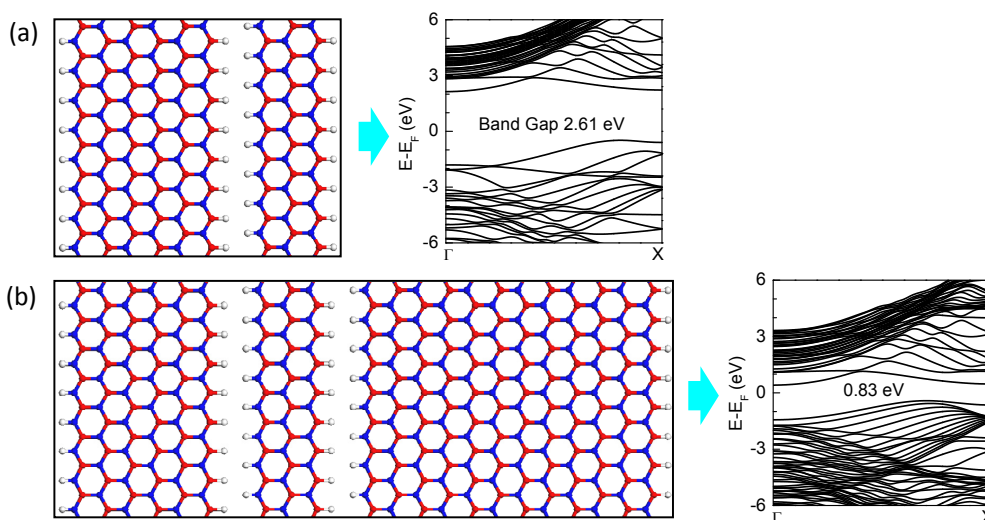


Fig. S3 Atomic and band structures of aligned nanoribbons composed of ZBNRs with different widths. (a) The aligned nanoribbons composed of a 6-ZBNR and a 3-ZBNR; the calculated band gap value is 2.61 eV, close to the gap of 2.57 eV in the 6-ZBNR-2. (b) The aligned nanoribbons composed of a 6-ZBNR, a 3-ZBNR and a 12-ZBNR; the calculated band gap value is 0.83 eV, close to the gap of 0.88 eV in the 6-ZBNR-3.

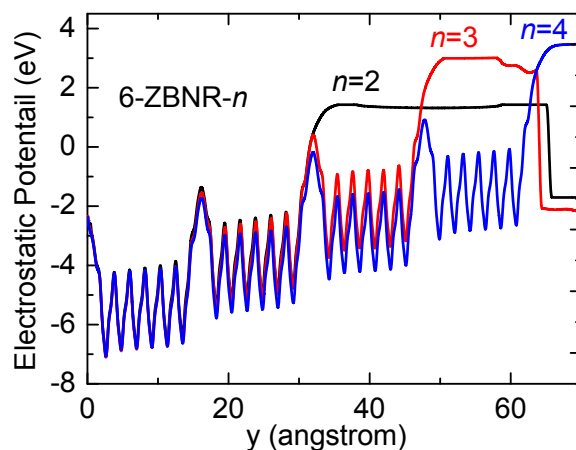


Fig. S4 Profile of averaged electrostatic potentials within the xz plane as a function of the y coordinate of the 6-ZBNR- n with $n=2, 3$ and 4 , respectively.

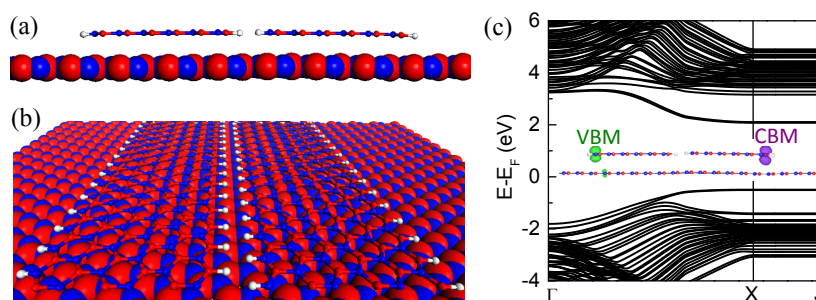


Fig. S5 Atomic and electronic structures for the 6-ZBNR-2 on a 2D h -BN sheet. (a,b) The front and planform views of the atomic structures. (c) The band structure of the system. The system has a direct band gap of 2.53 eV, almost identical to the band gap of a freestanding 6-ZBNR-2. Importantly, all the near-gap states are contributed by the 6-ZBNR-2, and the h -BN substrate remains insulating with a large indirect gap around 4.4 eV.

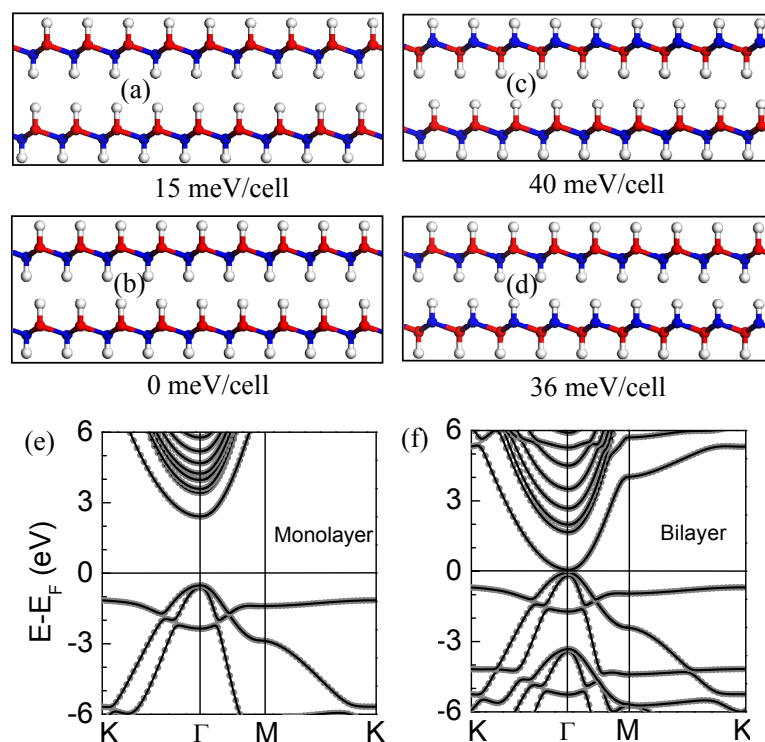


Fig. S6 Bilayer hydrogenated h-BN sheet with different interface structures. (a) B-end versus N-end interface with AA stacking, (b) B-end versus N-end interface with AB stacking, (c) N-end versus N-end interface with AB stacking and (d) B-end versus B-end interface with AB stacking. The energy below each figure is in relative to that of structure in (b). (e,f) GGA band structures of the (e) monolayer and (f) bilayer hydrogenated BN sheets. The Fermi level is set to zero.

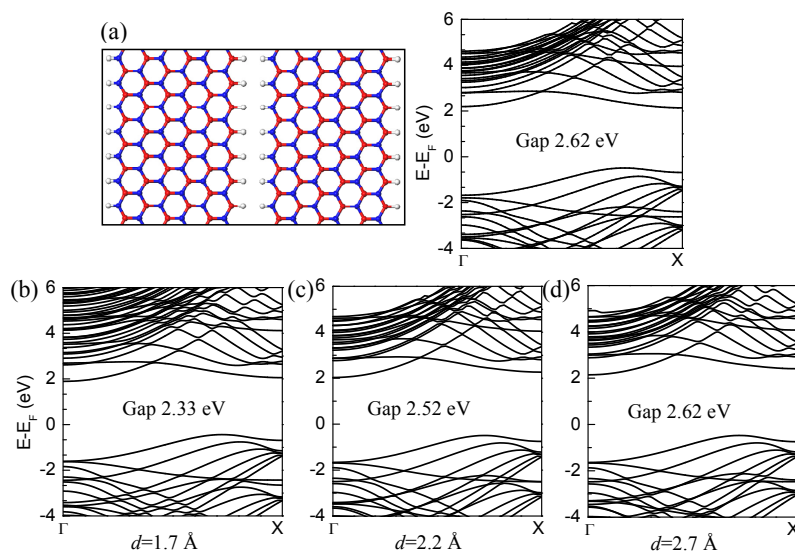


Fig. S7 Comparison of band structures of the 6-ZBNR-2 with different interface configurations as well as interface distance d . (a) The second-favorable structures together with their corresponding band structures. (c-d) The band structures of the 6-ZBNR-2 with (b) $d=1.7$, (c) $d=2.2$, (d) $d=2.7$, respectively.

These results suggest that the specific interface structure has a trivial effect on the band gap reduction in the aligned nanoribbons.

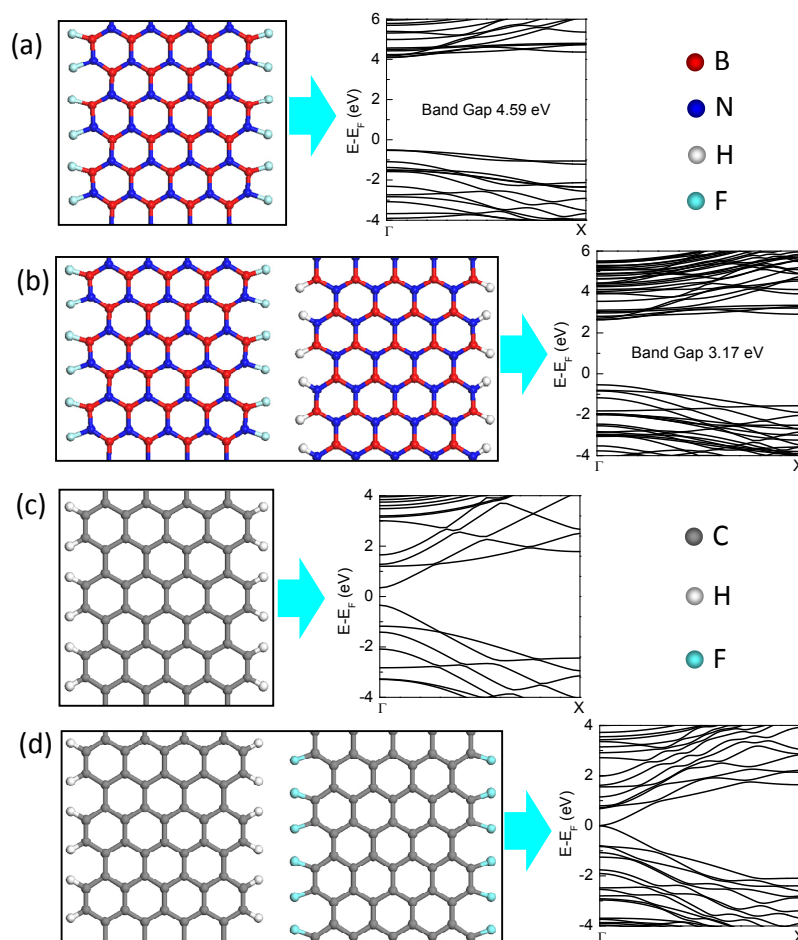


Fig. S8 Band gap reduction in aligned nonpolar armchair nanoribbons. (a,b) Atomic structures of the individual F-terminated armchair BNR and the aligned nanoribbons composed of an H-terminated and an F-terminated armchair BNRs, together with their band structures. (c) Atomic and band structures of the individual H-terminated armchair graphene nanoribbon. (d) Atomic and band structures of an aligned nanoribbons composed of an H-terminated and an F-terminated armchair graphene nanoribbons.

We find that the band gap of aligned armchair BNRs is reduced by 1.4 eV from that of individual armchair BNRs (Fig. S8a,b); whereas the band gap in aligned armchair graphene nanoribbon is even closed (Fig. S8d), in sharp contrast to individual ribbon units (Fig. S8c). The band gap reduction is attributed to the polar interface formed between the terminated H and F atoms, although both the H-terminated and F-terminated armchair ribbons are nonpolar.